

A β PP-induced UPR transcriptomic signature of glial cells to oxidative stress as an adaptive mechanism to preserve cell function and survival

Naïma Chalour^{1*}, Agathe Maoui^{2, 3, 4*}, Patrice Rat⁵, France Massicot⁵, Mélody Dutot⁵, Anne Marie Faussat⁶, Estelle Devevre², Astrid Limb⁷, Jean-Michel Warnet⁵, Jacques Tréton^{2, 3, 4}, Virginie Dinet^{2, 3, 4} and Frédéric Mascarelli^{2, 3, 4}

(1) Université des Sciences et Technologies d'Alger, laboratoire de Neurochimie/LBPO, FSB/USTHB, Alger, Algeria. (2) Centre de Recherche des Cordeliers, Université Paris Descartes, UMRS1138, Paris, F-75006 France; (3) INSERM, U1138, Paris, F-75006 France; (4) Université Pierre et Marie Curie - Paris6, UMRS 872, Paris, F-75006 France; (5) Faculté de Pharmacie de Paris, Toxicology lab UMR CNRS 8638, Université Paris Descartes, Sorbonne Paris Cité, F-75006 Paris, France; (6) IFR65, Institut de Recherche en Santé, Paris, F-75012; (7) University College London, Institute of Ophthalmology and Moorfields Eye Hospital, London, United Kingdom.

The last two authors are co-senior authors.

Running title: A β PP protects glial cells against oxidative stress

Corresponding authors: N.C.1 (naima.chalour@gmail.com) and F.M.2 (frederic.mascarelli@inserm.fr),

(1) Université des Sciences et Technologies d'Alger, laboratoire de Neurochimie/LBPO, FSB/USTHB, Alger, Algeria. (2) Centre de Recherche des Cordeliers, Université Paris Descartes, UMRS1138, Paris, F-75006 France.

ABSTRACT

Background: Alzheimer's disease (AD) and age-related macular degeneration (AMD) present similarities, particularly with respect to oxidative stress, including production of 4-Hydroxy-2-nonenal (HNE). AMD has been named the AD in the eye. The Müller cells (MC) function as a principal glia of the retina and maintain water/potassium, glutamate homeostasis and redox status. Any MC dysfunction results in retinal neurodegeneration. **Objectives:** We investigated the effects of HNE in human MC.

Results: HNE induced an increase of the reactive oxygen species associated with mitochondrial dysfunction and apoptosis. HNE induced endoplasmic reticulum (ER) stress (upregulation of GRP78/Bip, and the proapoptotic factor, CHOP). HNE also impaired expression of genes controlling potassium homeostasis (KCNJ10), glutamate detoxification (GS), and the visual cycle (RLBP1). MC adaptive response to HNE included upregulation of amyloid- β protein precursor (A β PP). To determine the role of A β PP, we overexpressed A β PP in MC. Overexpression of A β PP induced strong antioxidant and anti-ER stress (PERK downregulation and GADD34 upregulation) responses accompanied by activation of the prosurvival branch of the unfolded protein response. It was also associated with upregulation of major genes involved in MC-controlled retinal homeostasis (KCNJ10, GS, and RLBP1) and protection against HNE-induced apoptosis. Therefore, A β PP is an ER and oxidative stress responsive molecule, and is able to stimulate the transcription of major genes involved in MC functions impaired by HNE.

Conclusion: Our study suggests that targeting oxidative stress and ER stress might be a potential therapeutic strategy against glia impairment in AMD and AD, in light of the common features between the two pathologies.

Key words: A β PP, oxidative stress, glial cells, Alzheimer's disease, Age related macular degeneration, retina and apoptosis.

INTRODUCTION

The retina is derived from neural tube and thus an integral part of the central nervous system (CNS). The brain and the retina consume oxygen at a rate faster than any other organ in the body and have a high metabolic oxidative rate. Both tissues contain high levels of polyunsaturated fatty acids (PUFA) and redox transition metals and therefore are ideal targets for free radical attack. The main product formed from ω 6-PUFA under physiological conditions is the lipid peroxidation derived 4-hydroxynonenal (HNE). Lipid peroxidation is highly evident in neurodegenerative diseases and participates to the pathogenicity of oxidative stress in Alzheimer disease (AD) [1-4] and age-related macular degeneration (AMD) [5, 6]. AD is the most common form of dementia, and the number of cases is around 13-16 millions in the United States [7], while AMD is among the most frequent cause of progressive loss of central vision, with approximately 1.8 million affected individuals and 7 million people at risk of developing the disease in the US [8]. Age is a common risk factor for AD and AMD.

AMD is a complex, multifactorial disease (genetic and environmental factors) characterized by the degeneration of photoreceptors and retinal pigment epithelial (RPE) cells with (exudative form) or without (dry form) choroidal neovascularization. The only current treatment for the dry form of AMD based on the Age-Related Eye Disease Study is a mixture of micronutrients and anti-oxidants [9], and there are no drug treatments that can cure AD. AMD and AD have many parallel characteristics.

Amyloid- β ($A\beta$) is the main constituent of the plaques in the brain of AD patients and one of the major components of the drusen deposits in the retina of AMD patients [10]. We have previously shown that $A\beta$ (1-42) induces retinal oxidative stress associated with RPE cell alteration, HNE production in photoreceptors followed by photoreceptor apoptosis [11, 12]. Of note, anti- $A\beta$ immunotherapy reduces retinal pathologies in an AMD mouse model [13]. In AD patients, $A\beta$ deposits associated with retinal abnormalities and visual deficits, and ocular manifestations have been detected in the retina earlier than in the brain [14, 15]. The number and size of retinal $A\beta$ deposits correlate with brain pathology in a mouse model of AD and AD patients [15]. Therefore, it has been suggested that retina can be used as a biomarker of AD diagnosis and progression, and depicting retinal changes can allow managing of AD at very early stages [16, 17]. Additional common features between AD and AMD include reactive gliosis, oxidative stress, endoplasmic reticulum (ER) stress and inflammation. Due to the parallels between the two pathologies, AMD has been recently named the dementia of the eye [18] or the AD in the eye [19]. Therefore, it has been postulated that characterizing the pathogenic pathways of AMD, may give insights both for better understanding the pathogenic pathways and developing future therapeutic targets to AD.

The membranes of both brain astrocytes and retinal glial Müller cells (MC), the major type of glial cells in the retina, bear numerous pumps, channels and transporters that are responsible for water, ion, metabolite and neurotransmitter homeostasis [20-22]. Any deficit in MC function results in retinal neurodegeneration and visual impairment. In AMD, oxidative stress contributes to the induction or progression of MC gliosis [21, 23], which occurs before photoreceptor degeneration appears [24]. Increased levels of HNE have been detected in the retinas of patients with AMD and the brain of AD patients. HNE has been shown to mediate photoreceptor apoptosis in animal models of AMD [25-28]. HNE also induces RPE cell death in culture [29, 30]. The protective mechanism against HNE-induced oxidative stress has been elucidated in RPE cells [31, 32] and the transcriptomic responses to HNE of RPE cells were identified [33, 34]. Although MC responses to HNE are central for photoreceptor and RPE survival in AMD, no study has been undertaken to characterize the molecular mechanism of HNE-induced MC death. Moreover, the protective pathways against HNE-mediated toxicity and the transcriptomic response to the HNE-induced oxidative stress in MC have not been investigated. HNE may also induce endoplasmic reticulum (ER) stress. It has been postulated that ER stress-triggered transcriptional reprogramming plays fundamental roles in the initiation and progression of neurological disorders [35, 36]. The role of ER stress in AMD remains to be elucidated [37, 38]. Oxidative stress and ER stress increase production of Amyloid- β protein precursor (A β PP). The apparently conflicting results regarding the proapoptotic role of A β PP in lethal ER stress leaves its role unclear. Some studies report that A β PP overexpression is associated with upregulation of the pro-apoptotic factor CHOP and with cell death in cell cultures [39, 40], others find that overexpression of A β PP protects neurons from prolonged ER stress and cell death in cell cultures [41, 42] and from acute and chronic excitotoxic brain injuries [43]. Although several studies observed upregulation of A β PP expression in MC of degenerating retinas [44-46], no study has yet investigated the effects of A β PP overexpression on MC and in retinal degeneration.

The aim of this study was to investigate the effects of HNE on MC and determine the potential protective role of A β PP against HNE. We show that HNE induced apoptosis of MC, associated with oxidative stress and ER stress. Stable overexpression of A β PP induced a strong antioxidant and anti-ER stress, protecting MC against HNE-induced apoptosis. These results are discussed in light of the common features between AD and AMD and other recently published data.

MATERIALS AND METHODS

MC cultures and treatment: The human MIO-M1 (Moorfields/institute of Ophthalmology- Müller 1) cell line was established previously [47]. The cell line was confirmed to be human and no evidence of cross-species contamination was found. The STR testing results reported for the cell line are as follows: amelogenin (X, Y), CSF1PO (13, 14), D13S317 (13), D16S539 (11, 12), D5S818 (12, 13), D7S820 (7, 9),

TH01 (6, 9.3), TPOX (6, 9), and vWA (15, 19). The cells were maintained as an adherent cell line in 75-cm² tissue culture flasks in D-MEM (GlutaMAX; Invitrogen) supplemented with 10% heat-decomplemented fetal calf serum (FCS; GibcoBRL) and penicillin/streptomycin (Invitrogen). We applied HNE-mediated oxidative stress in 10% FCS-containing medium, inducing it as follows: Cells were seeded in 24-well polystyrene plates (Nalgenunc) at a density of 20,000 cells per cm² in complete culture medium for 24 h. Cells were then treated with the appropriate concentration of HNE. Control cell cultures consisted of cells cultured in complete culture medium in the absence of HNE. Time zero of the kinetics corresponds to the moment of treatment with HNE.

To analyze the role of c-Jun NH₂-terminal kinase (JNK) signaling, the specific inhibitor of JNK (SP600125, Calbiochem) was added 30 minutes before HNE treatment and then in combination with HNE. Antioxidant defense signaling was stimulated 1 hour before HNE treatment, with the following chemicals: N-acetylcystein (NAC), glutathione monoethyl ester (GME), resveratrol, and trolox (Calbiochem). Stock solutions of each inhibitor were prepared in DMSO and diluted in DMEM for a final DMSO concentration not exceeding 0.1% in test solutions (a concentration with no effect on cell death).

Measurement of intracellular oxidation: The dichlorodihydrofluoresceindiacetate (H₂DCFDA, Interchim) method was used to measure extracellular reactive oxygen species (ROS) levels, as previously described [48]. Cells were incubated with 1 µM H₂DCFDA for 15 min at 37°C, collected in 500 µl 1% PAF, and analyzed by flow cytometry according to manufacturer's recommendations (Epics ALTRA; Beckman Coulter). We adjusted cell density at 1.5 x 10⁶ cells/mL for treatment. Then, we adjusted at least 10,000 single cell events per sample in the analysis gate.

Measurement of intracellular potential with the Alamar Blue test: Intracellular redox status, correlated with redox potential, was evaluated with Alamar Blue[®] dye (Sigma-Aldrich). Cells treated with or without HNE for the indicated times were incubated with Alamar Blue (20 µL) for 6 h. The Alamar Blue fluorescence was then measured at λ_{exc}=535 nm, λ_{em}=600 nm. Measurement of mitochondrial transmembrane potential: Mitochondrial transmembrane potential was measured with the JC-1 probe (Invitrogen). Cells treated with or without HNE for the indicated times were incubated with the dye solution (6.5 µg/mL in PBS) for 15 min and fluorescence was read at λ_{exc}=485 nm, λ_{em}=520 nm.

Measurement of mitochondrial redox potential: Mitochondrial redox potential was assessed spectrophotometrically with an MTT assay (Sigma-Aldrich), as previously described [48]. Measurement of mitochondrial cardiolipin: Cardiolipin release serves as a marker of change in the mitochondrial inner membrane. This parameter was evaluated with the 10-N-nonyl acridine orange probe (Invitrogen). Cells treated with or without HNE for the indicated times were incubated with the dye solution (10 µM in

culture medium) for 30 minutes. The dye was extracted from cells with a solution of acetic acid-ethanol, and fluorescence was read at $\lambda_{exc}=490$ nm, $\lambda_{em}=530$ nm.

Assays for cell viability: Cell viability was assessed by: 1) counting trypan blue-excluding cells after adding 0.5% trypan blue; 2) monitoring LDH release into the culture, with a cytotoxicity detection kit (Roche Diagnostics, Meylan, France), as previously described [48]. Cell cycle progression and cell apoptosis analysis: We analyzed the cell cycle of cells with propidium iodide (PI), determining the cell DNA content after 24 h. The stained cells were analyzed by flow cytometry. To quantify the effect of HNE on cell cycle especially on sub-G1 population (apoptotic cells), we adjusted cell density 1.5×10^6 cells/mL for treatment. Then, we adjusted at least 10,000 single cell events in the analysis gate. We analyzed apoptotic cell death by terminal dUTP nick end labeling (TUNEL) (PCD kit, Boehringer), carried out according to the manufacturer's recommendations. We observed and counted TUNEL-positive cell nuclei in three different fields within an ocular grid using a 25X objective with a Leitz Aristoplan microscope. A minimum of 200 cells was counted per cell treatment. We calculated the percentages of apoptotic cell nuclei in comparison to the untreated control cells.

Cell adhesion and proliferation: Cells were allowed to attach to the surface of the plastic dishes at 37 °C, 5% CO₂ for the indicated times. Then, non-adherent cells were removed from the culture medium with gentle washing with PBS. After mild trypsinization, the number of attached MC was counted at the indicated times using a cell counting plate of Malassez after staining with trypan blue dye. A minimum of 100 cells was counted per sample.

Cell transfection: Cells were transfected with pcDNA3APP containing the human APP695 coding sequence under control of the SV40 promoter and enhancer (kindly provided by Dr. L. Désiré, ExonHit Therapeutics, Paris, France) by the CaPO₄ method. Briefly, 500 ng plasmid DNA was diluted in 75 μ L of 0.25 M CaCl₂ and added dropwise to 75 μ L of 2xHeBS (280 mM NaCl, 1.4 mM Na₂HPO₄, 50 mM HEPES, pH 7.1). After an overnight incubation of cells with the transfection solution, cells were cultured for 24 h in fresh medium. G418 selection (500 μ g/mL, Sigma) was started 72 h posttransfection and continued for 3 weeks. The empty pcDNA3 vector was used as a control.

Western blot analysis: Cells were washed twice in PBS, lysed in ice-cold lysis buffer (50 mM TrisHCl, pH 7.5, 100 mM NaCl, 50 mM NaF, 5 mM EDTA, 40 mM β -glycerophosphate, 0.2 mM sodium orthovanadate, 1 μ g/mL leupeptin, and 1 μ M pepstatin). The lysates were then resolved by SDS-PAGE and transferred by electroblotting to PVDF filters. Polyclonal antibodies: anti-phospho-JNK antibody (Thr183 and Tyr185, dilution 1: 1000, Cell Signaling Technology), anti-cleaved caspase 3 and anti cleaved caspase 9 antibodies (dilution 1:1000, Cell Signaling Technology). The primary antibodies were detected

with a horseradish peroxidase-conjugated antibody. We used ECL substrate to detect the secondary antibody, according to the manufacturer's instructions.

Quantitative real-time polymerase chain reaction (qRT-PCR): Total RNA from cells was isolated with the Qiagen extraction kit (RNeasy Plus Mini kit) according to the manufacturer's instructions, and SuperScript II Reverse Transcriptase (Invitrogen) was used to reverse transcribe 2 µg of mRNA. Amplification reaction assays contained 1x SYBR Green PCR Mastermix. A hot start at 95°C for 5 min was followed by 40 cycles at 95°C for 15 seconds and 60°C for 1 min with the 7300 SDS thermal cycler (Applied Biosystems). Controls with no reverse transcriptase were run for each assay to confirm the lack of genomic DNA contamination. Control qRT-PCR reactions were performed without cDNA templates. The standard curve method (Prism 7700 Sequence Detection System; ABI User Bulletin number 2) was used for relative quantification of gene expression. At least two experiments were conducted for each gene and sample. At each experiment, each individual sample was run in triplicate wells and the Ct of each well was recorded at the end of the reaction. The average and standard deviation of the three Cts was calculated. Gene expression levels were normalized to GAPDH for each treated MC sample, and calculated relative to untreated MC sample (control) with the following equation: relative expression = $2^{-(\text{sample}\Delta\text{Ct}-\text{control}\Delta\text{Ct})}$ where $\Delta\text{Ct} = \text{mean Ct}(\text{target}) - \text{mean Ct}(\text{GAPDH})$.

Statistical Analyses: All experiments were performed in triplicate. Statistical analyses were performed with Graph PAD Software. We tested for normality with the Kolmogorov–Smirnov test.

Differences between groups were compared with one-way ANOVA tests for cell viability and Student's t-test for gene expression levels. Data are expressed as means \pm SD, and the differences were considered statistically significant at $p < 0.05$.

RESULTS

HNE-mediated oxidative stress induced mitochondrial dysfunction in MC

We investigated the effects on MC cultures of a single treatment with exogenous HNE. A very slight increase in the production of intracellular ROS measured by H2DCFDA was detected at the low concentration of 2 µM HNE (increased ROS production by 17% compared with treatment by the vehicle alone), whereas 20 µM HNE induced a large increase in ROS production (180%) after 6 h of

treatment (Fig. 1A). Cell treatment with HNE induced a significant dose-dependent decrease (up to 65%) in intracellular redox potential evaluated with Alamar Blue, after a 24-h culture period (Fig. 1B).

The MTT colorimetric assay showed that HNE treatment caused a rapid time- and concentration dependent alteration in the MC' mitochondrial redox potential at doses above 10 µM (Fig. 1C).

Moreover, the marked reduction in the JC-1 ratio induced by cell treatment with 20 and 50 µM HNE (after 24 h, decreases of 25 and 33%, respectively) indicated that HNE decreased $\Delta\psi_m$ (Fig. 1D). At similar concentrations, HNE increased cardiolipin release (after 24h, increases of 75% and 122%, respectively) (Fig. 1E), demonstrating changes in the mitochondrial inner membrane, notably the

modification of membrane fluidity.

MC respond to HNE by induction of the antioxidant NRF2 pathway, and the proapoptotic and autophagic branches of the UPR

In order to identify gene pathways that might be affected by HNE in MC, we compared gene expression in MC treated with 20 μ M HNE and in control MC at early stages of oxidative stress (within 6 h of MC cell treatment with HNE). We used qRT-PCR analysis to test 26 genes related to oxidative and ER stress (Table 1). A modest upregulation was observed in the expression of the antioxidant transcription factor NRF2 (by a factor of 1.3), and the two NRF2 target enzymes, aldo ketoreductase family 1 member C1 (AKR1C1) and the glutamate-cysteine ligase catalytic subunit (GCLC), the first rate-limiting enzyme of glutathione (GSH) synthesis (by factors of 1.9 and 2.3, respectively). The expression of other major antioxidant enzymes, including catalase, superoxide dismutase (SOD) 1, SOD2, and glutathione S-transferase A4 (GSTA4), was not affected. Among these genes belonging to the three branches of the UPR, the proapoptotic transcription factor C/EBP homologous protein (CHOP) was the most significantly affected by HNE (upregulation by a factor of 2.7). Upregulation (by a factor of 2.2) of the spliced form of XBP1 (X-box binding protein 1), XBP1s, following cell exposure to HNE was also observed. GRP78 expression was consistently upregulated (by a factor of 1.5) following cell exposure to HNE. But HNE did not affect any of the major ER associated protein degradation (ERAD) components. In contrast, it did upregulate (by a factor of 2.1) MAP1-LC3, the major autophagic gene. Interestingly, HNE upregulated (by a factor of 1.4) expression of mRNA for all three spliced A β PP isoforms as well as expression of the glial A β PP isoform, APP770 (by a factor of 1.3) (Table 1).

MC elicit a specific transcriptional program in response to HNE, with the induction of anti inflammatory genes, together with impairment of retinal homeostasis genes

Both oxidative and ER stress are thought to be implicated in retinal degeneration, partly through their impairment of the expression of genes involved in specific retinal cell functions. MC elicit a specific transcriptional program in response to HNE, with the induction of anti-inflammatory genes, together with impairment of genes involved in K⁺ and glutamate homeostasis (Supplementary Table S1).

HNE induced GSH-dependent and caspase-associated apoptosis of MC

We next sought to determine whether HNE-induced mitochondrial dysfunction, oxidative stress and ER stress, might damage MC. The LDH assay showed that 2 μ M HNE had no effects on LDH release, but that HNE concentrations of 20 μ M up to 50 μ M induced a significant time-dependent

increase in the release of LDH activity (Fig. 2A). The trypan blue-excluding cell assay showed that 2 μ M HNE did not significantly affect MC viability (Fig. 2B). MC were quite resistant to 20 μ M of HNE: 50% of the cells survived after 48 h (Fig. 2B). In contrast, after 6 h with 50 μ M HNE, almost all the MC died. Treatment with HNE at 20 and 50 μ M for 24 h resulted in the accumulation of cells in the sub-G1 phase of the cell cycle (apoptotic cells) from 3.5-5% in the untreated control cells to 27.7 and 52.0%, respectively (Fig. 2C). Moreover, we observed numerous TUNEL-positive cell nuclei in cultures treated for 24 h with 20 μ M HNE (33.1%), but detected none in untreated control MC (Fig. 2D), confirming HNE-induced MC apoptosis. Intracellular production of ROS in MC was inversely correlated with cell survival during HNE treatment (Supplementary Fig. S1A). HNE induces glutathione-dependent cell death (Supplementary Fig. S1B) and activated caspase-associated apoptosis of MC (Supplementary Fig. S1C).

A β PP protected MC from HNE-induced cell death, independently from JNK

At moderate levels of sustained overexpression, human A β PP protects cell lines and transgenic mice against oxidative stress and increases resistance to excitotoxicity [39-43]. However, the exact mechanism of these protective effects remains largely unknown. In line with these findings and our data, we hypothesized that upregulation of A β PP is an adaptive process to protect MC against lethal HNE-induced oxidative stress. To test this hypothesis, we stably transfected MC with the pc-DNA APP695 expression vector (MCapp cells) (Supplementary Fig. S2A). Overexpression of A β PP in MC did not affect either cell adhesion (Supplementary Fig. S2B) or cell proliferation (Supplementary Fig. S2C). A β PP overexpression significantly reversed the mitochondrial redox potential decrease in MC after HNE treatment compared to control cells (MC pc) (Fig. 3A) and halved the percentage of cell death after treatment with 20 μ M HNE at both 24 and 72 h, according to the trypan blue-excluding cell count (Fig. 3B).

The death-inhibiting function of A β PP involved inhibiting JNK [40]. We therefore hypothesized that JNK inhibition may be part of the protective mechanism of action of A β PP in HNE-treated MC. Surprisingly, JNK signaling was not activated in MCapp compared with control cells and MC treatment with the JNK inhibitor, SP600125, had no protective effect against HNE-induced cell death (Supplementary Fig. S3).

A β PP induced the ER-associated degradation of misfolded protein (ERAD) system and a specific antioxidant response, and restored expression of major genes involved in retinal homeostasis

We hypothesized that A β PP might protect MC from HNE through a specific anti-oxidative transcriptional program. Therefore, we compared gene expression in MCapp cells and MCpc cells, using qRT-PCR analysis to test 20 genes related to the three main processes altered by HNE treatment

–UPR, ERAD, and oxidative stress – and 4 genes related to specific MC functions (Table 3). MCapp cells expressed 18 genes differentially (18/24, 75%), suggesting that MC have a strong transcriptional response associated with A β PP overexpression. The gene coding for the translation repressor PERK of the proapoptotic branch of the UPR and ATF6 were the only two genes downregulated in MCapp (by factors 1.9 of and 1.3, respectively). Conversely, the PERK signaling inhibitor GADD34, which is critical for ER stress relieve was one of the genes most highly upregulated (by a factor of 2.4) after A β PP overexpression. Consistently, the expression of ATF4 involved in GADD34 induction and resistance to oxidative stress was upregulated (increased by 1.4). The protective gene against ER stress and oxidative stress, XBP1, and its spliced form, XBP1s were also upregulated (increased by factors of 2.1 and 4, respectively). The expression of CHOP, a central mediator of ER stress-induced apoptosis was not affected. Moreover, the two major ER chaperones involved in ERAD, CNX and Hrd1, were upregulated (by factors of 2.1 and 1.4, respectively) as well as genes coding for EDEM1 and EDEM2 (by factors of 1.8 and 2.3, respectively). The latter two proteins interact with CNX to help translocate misfolded proteins to the proteasome for degradation. This data clearly indicates that overexpression of A β PP was able to stimulate the transcription of major UPR genes involved in resistance to oxidative stress and ERAD genes.

Among the antioxidant genes, NRF2 was the most highly upregulated gene after A β PP overexpression (by a factor of 7.5) (Table 3). The NRF2-driven antioxidant enzymes, GCLC (implicated in GSH synthesis) and GSTA4 (catalyze the conjugate addition of reduced GSH to HNE), were consistently upregulated (by factors of 2.0 and 2.7, respectively) in MCapp cells. Upregulation of catalase (increased by a factor of 3.7) was also consistent with induction of both NRF2 and XBP1 in MCapp cells and protective effects of the GSH analog against HNE in MC (Supplementary Fig. S1B). Both oxidative and ER stress are thought to be implicated in retinal degeneration, partly through their impairment of the expression of genes involved in MC cell-associated retinal functions. Therefore, we investigated whether overexpression of A β PP also affected the expression of genes involved in specific MC cell functions and which specific genes had their expression impaired after HNE treatment. A β PP overexpression was associated with an upregulation of the expression of four key genes coding for the main MC functional proteins, two involved in K⁺ transport (KCNJ2, which increased by a factor of 5.2, and KCNJ10, by a factor of 5.1), one in glutamate detoxification (GS increased by a factor of 2.1), and one in the visual cycle (RLBP1, by a factor of 1.7) (Table 3). This data clearly indicates that overexpression of A β PP was able to stimulate the transcription of major genes involved in MC functions impaired by HNE treatment.

DISCUSSION

The UPR transcriptomic signature associated with the antioxidant role of A β PP: similarities between AMD and AD

Several studies observed neurotrophic and neuroprotective effects of A β PP [49-51]. The role of A β PP in retinal degeneration was never investigated. Our study demonstrates, for the first time to our knowledge, the glioprotective effects of A β PP by showing that overexpression of A β PP after stable transfection of A β PP cDNA protected MC from oxidative stress-mediated HNE-induced apoptosis. The antioxidant activity of A β PP was associated with a specific antioxidant transcriptomic signature (summarized in the schema, Fig. 4): NRF2 was the most highly upregulated gene in MC that overexpressed A β PP (by a factor of 7.5). In the retina, NRF2 is expressed prominently in MC. Therefore expression of the NRF2-driven genes, CAT, GSTA4 and GCLC, was consistently upregulated in A β PP-overexpressing MC. We hypothesized that upregulation of NRF2 and NRF2 driven antioxidant enzymes might be part of the protective mechanism induced by A β PP overexpression in MC. Consistent with our work and this hypothesis, recent studies have reported that: 1) NRF2-deficient mice develop AMD-like retinal pathology with photoreceptor loss [52]; 2) upregulation and activation of NRF2 protect RPE cells [53] and photoreceptors [54, 55] against oxidative stress in in vitro and in vivo models of retinal degeneration; 3) pharmacological activation of NRF2 inhibited gliosis of MC in an in vivo model of retinal degeneration and increased NRF2 responsive antioxidants in cultured MC [56]. Interestingly, several studies also showed pivotal role for NRF2 in the brain astrocytes. Overexpression of NRF2 activation in astrocytes confers protection from oxidative stress-induced death on neurons [57]. NRF2 has also been shown to play a major role against AD features in AD mouse models. Genetic ablation of NRF2 increases the AD-like pathology in the APP/PS1 Δ 9 mouse model, while intrahippocampal injection of a lentiviral vector expressing NRF2 improves spatial learning in the APP/PS1 mouse model of AD [58, 59]. A reduction in astrocytic but not microglial activation is observed in the brain of NRF2-injected APP/PS1 mouse [59]. Although, the exact mechanisms of MC/astrocytes-mediated neuroprotection remain unclear, targeting NRF2 or NRF2-regulated genes could be considered as a neuroprotective strategy in AMD and AD.

Protein misfolding-induced ER stress plays a fundamental role in the oxidative stress associated pathogenesis of several neurodegenerative diseases, including AMD and AD. We showed here that HNE upregulates the expression of GRP78/BiP, CHOP, XBP1, XBP1s and GADD34 in MC, changes indicative of a strong ER stress in these cells (summarized in the schema, Fig.4). The antioxidant activity of A β PP was also associated with a specific UPR, ERAD and autophagy transcriptomic signature (summarized in the schema, Fig. 4). The exact mechanisms of MC in the protection of retinal cells (photoreceptors or RPE cells) during AMD are unclear. Potential protective

mechanisms exist, such as the UPR although demonstration of the incidence of ER stress in AMD is still lacking. A β PP overexpression was associated with a pronounced upregulation (quadrupling) of XBP1s, which activates a subset of UPR genes participating in ERAD to relieve ER stress. We detected consistent upregulation of four ERAD genes, CNX, EDEM1, EDEM2, and HRD1, in A β PP overexpressing MC. This finding strongly suggested the hypothesis that the protective effects of A β PP might be mediated partly through the induction of ERAD genes, such as XBP1, to reduce the protein unfolding in HNE-treated MC. Consistent with our work and this hypothesis, recent studies have reported that: 1) XBP1s levels increase in the degenerating retina of a *Drosophila* model for photoreceptor degeneration [60]; 2) overexpression of XBP1 protects against hydroquinone- and cigarette smoke extract (CSE)-induced apoptosis in RPE cells [61, 62]; 3) a mouse line that lacks XBP1 only in RPE cells exhibited characteristic features of AMD, including, apoptosis of RPE cells, decreased number of photoreceptors, shortened photoreceptor outer segment and deficit in visual function [63]. What is worthy of note, however, is the downregulation of XBP1 in the brain of AD patients and mouse models of AD [64], suggesting that alteration of ERAD might contribute to development or progression of AD. Moreover, in terms of functional studies, a neuro-protective activity of XBP1 was proposed on two fly models of AD [65, 66].

Interestingly, XBP1-induced activation of the UPR requires upregulation of NRF2 in CSE treated RPE cells [62], suggesting a direct link between oxidative stress and ER stress in AMD. This is in agreement with the upregulation of both NRF2 and XBP1 in A β PP-overexpressing MC. The link between ER and oxidative stress has been also observed in AD. The levels of NRF2 and XBP1 are significantly increased in the brain cortex of a mouse model of AD, compared to age-matched WT [67]. Moreover, the role of XBP1-activated UPR genes, such as EDEM2, and HRD1, may be part of the protective effect of A β PP because overexpression of these two genes protects against misfolded rhodopsin-induced photoreceptor cell death in a *Drosophila* model of photoreceptor degeneration [68]. Therefore, A β PP overexpression might regulate a coordinated expression of a battery of cytoprotective genes, including those of the prosurvival branch of the UPR and the anti-oxidant defense, leading to the direct cellular protection in MC. In a mouse model of Leber congenital amaurosis, the most severe retinal dystrophy in early childhood, a rapid and massive S-cone degeneration occurs through an ER stress [69]. Very recently, it has been shown that overexpression of A β PP in mice preserve S-cone function [70]. The role of A β PP in retinal degeneration deserves investigation.

CONCLUSION

In conclusion, our data show that HNE, which accumulates in the retinas of patients with AMD, induced mitochondrial dysfunction and MC apoptosis, through a complex transcriptional response related to oxidative stress, ER stress, inflammation, amyloidogenesis and retinal homeostasis.

The transcriptional responses to HNE of MC and RPE cells differ. These results together with the resistance against HNE observed in photoreceptors and RPE cells, suggest that the neurodegeneration in retina may result secondary to oxidative stress-induced impairment of MC homeostatic functions. Overexpression of A β PP stimulated the expression of some HNE-altered master genes involved in prosurvival retinal functions, including antioxidant, UPR, and glutamate- and osmohomeostasis; it also protected MC from HNE-induced cell death. Of note, some of these genes have been shown to play a role in both AMD and AD (reactive gliosis, oxidative stress, ER stress and inflammation). Because AMD has been recently named the dementia of the eye or the AD in the eye, our findings thus suggest that therapeutic strategies targeting these genes might be useful in treating neurodegeneration mediated by oxidative stress and ER stress in AMD and AD.

SUPPLEMENTARY MATERIAL Supplementary material is available on the publisher's web site along with the published article.

CONFLICT OF INTEREST The authors confirm that this article content has no conflict of interest.

ACKNOWLEDGEMENTS

Grant support: Supported by the Ministère de la Recherche (Naïma Chalour and Agathe Maoui) and the Agence Nationale de la Recherche (P. Rat, F. Massicot, M. Dutot, J-M. Warnet, V. Dinot and F. Mascarelli). We thank Dr. I. El Zaoui (University of Lausanne, 1011 Lausanne Switzerland) and Drs. I. Jaadane and A. Torriglia (Centre de Recherche des Cordeliers, Paris, France) for critically reading the manuscript and for stimulating discussions.

REFERENCES

- 1- Reed TT. Lipid peroxidation and neurodegenerative disease. *Free Radic Biol Med* 51(7):1302-19 (2011)
- 2- Sultana R, Perluigi M, Allan Butterfield D. Lipid peroxidation triggers neurodegeneration: a redox proteomics view into the Alzheimer disease brain. *Free Radic Biol Med* 62:157-69 (2013)
- 3- Praticò D. Evidence of oxidative stress in Alzheimer's disease brain and antioxidant therapy: lights and shadows. *Ann N Y Acad Sci* 1147:70-8 (2008)
- 4- Markesbery WR. Oxidative stress hypothesis in Alzheimer's disease. *Free Radic Biol Med*.23(1):134-47 (1997)
- 5- Jarrett SG, Boulton ME. Consequences of oxidative stress in age-related macular degeneration. *Mol Aspects Med* 33(4):399-417 (2012)
- 6- Beatty S, Koh H, Phil M, Henson D, Boulton M. The role of oxidative stress in the pathogenesis of age-related macular degeneration. *Surv Ophthalmol* 45(2):115-34 (2000)

- 7- Hebert LE, Scherr PA, Bienias JL, Bennett DA, Evans DA. Alzheimer disease in the US population: prevalence estimates using the 2000 census. *Arch Neurol* 60(8):1119-22 (2003)
- 8- Friedman DS, O'Colmain BJ, Muñoz B, Tomany SC, McCarty C, de Jong PT, et al. Eye Diseases Prevalence Research Group. Prevalence of age-related macular degeneration in the United States *Arch Ophthalmol* 122(4):564-72 (2004)
- 9- Chew EY, Clemons TE, Agrón E, Sperduto RD, Sangiovanni JP, Kurinij N, et al. Age-Related Eye Disease Study Research Group. Long-term effects of vitamins C and E, β -carotene, and zinc on age-related macular degeneration: AREDS report no. 35. *Ophthalmology* 120(8):1604-11 (2013)
- 10- Ohno-Matsui K. Parallel findings in age-related macular degeneration and Alzheimer's disease. *Prog Retin Eye Res* 30(4):217-38 (2011)
- 11- Bruban J, Glotin AL, Dinét V, Chalour N, Sennlaub F, Jonet L, An N, Faussat AM, Mascarelli F. Amyloid-beta(1-42) alters structure and function of retinal pigmented epithelial cells. *Aging Cell* 8(2):162-77 (2009)
- 12- Bruban J, Maoui A, Chalour N, An N, Jonet L, Feumi C, Tréton J, Sennlaub F, Behar-Cohen F, Mascarelli F, Dinét V. CCR2/CCL2-mediated inflammation protects photoreceptor cells from amyloid- β -induced apoptosis. *Neurobiol Dis* 42(1):55-72 (2011)
- 13- Ding JD, Lin J, Mace BE, Herrmann R, Sullivan P, Bowes Rickman C. Targeting age-related macular degeneration with Alzheimer's disease based immunotherapies: anti-amyloid-beta antibody attenuates pathologies in an age-related macular degeneration mouse model. *Vision Res* 48(3):339-45 (2008)
- 14- Parnell M, Guo L, Abdi M, Cordeiro MF. Ocular manifestations of Alzheimer's disease in animal models. *Int J Alzheimers Dis* 2012:786494 (2012)
- 15- Koronyo-Hamaoui M, Koronyo Y, Ljubimov AV, Miller CA, Ko MK, Black KL, et al.. Identification of amyloid plaques in retinas from Alzheimer's patients and noninvasive in vivo optical imaging of retinal plaques in a mouse model. *Neuroimage* 54 Suppl 1:S204-17 (2011)
- 16- Sivak JM. The aging eye: common degenerative mechanisms between the Alzheimer's brain and retinal disease. *Invest Ophthalmol Vis Sci* 54(1):871-80 (2013)
- 17- Jindal V. Interconnection between brain and retinal neurodegenerations. *Mol Neurobiol* 51(3):885-92 (2015)
- 18- Ratnayaka JA, Serpell LC, Lotery AJ. Dementia of the eye: the role of amyloid beta in retinal degeneration. *Eye (Lond)* 29(8):1013-26 (2015)
- 19- Kaarniranta K, Salminen A, Haapasalo A, Soininen H, Hiltunen M. Age-related macular degeneration (AMD): Alzheimer's disease in the eye? *J. Alzheimers Dis* 24(4):615-31 (2011)
- 20- Reichenbach A, Bringmann A. New functions of Müller cells. *Glia* 61(5):651-78 (2013)

- 21- Bringmann A, Pannicke T, Grosche J, Francke M, Wiedemann P, Skatchkov SN, et al. Muller cells in the healthy and diseased retina. *Prog Retin Eye Res* 25(4):397-424 (2006)
- 22- Rodríguez-Arellano JJ, Parpura V, Zorec R, Verkhratsky A. Astrocytes in physiological aging and Alzheimer's disease. *Neuroscience* 323:170-82 (2016)
- 23- Bringmann A, Iandiev I, Pannicke T, Wurm A, Hollborn M, Wiedemann P, et al. Cellular signaling and factors involved in Muller cell gliosis: neuroprotective and detrimental effects. *Prog Retin Eye Res* 28(6):423-51 (2009)
- 24- Diloreto DA Jr, Martzen MR, del Cerro C, Coleman PD, del Cerro M. Müller cell changes precede photoreceptor cell degeneration in the age-related retinal degeneration of the Fischer 344 rat. *Brain Res* 698:1–14 (1995)
- 25- Tanito M, Haniu H, Elliott MH, Singh AK, Matsumoto H, Anderson RE. Identification of 4-hydroxynonenal-modified retinal proteins induced by photooxidative stress prior to retinal degeneration. *Free Radic Biol Med* 41:1847-59 (2006)
- 26- Marchette LD, Thompson DA, Kravtsova M, Ngansop TN, Mandal MN, Kasus-Jacobi A. 2010. Retinol dehydrogenase 12 detoxifies 4-hydroxynonenal in photoreceptor cells. *Free Radic Biol Med* 48 (1):16-25 (2010)
- 27- Shen JK, Dong A, Hackett SF, Bell WR, Green WR, Campochiaro PA. Oxidative damage in age related macular degeneration. *Histol Histopathol* 22: 1301-1308 (2007)
- 28- Ethen CM, Reilly C, Feng X, Olsen TW, Ferrington DA. Age-related macular degeneration and retinal protein modification by 4-hydroxy-2-nonenal. *Invest Ophthalmol Vis Sci* 48:3469-79 (2007)
- 29- Kaarniranta K, Ryhänen T, Karjalainen HM, Lammi MJ, Suuronen T, Huhtala A, et al. Geldanamycin increases 4-hydroxynonenal (HNE)-induced cell death in human retinal pigment epithelial cells. *Neurosci Lett* 2:185-90 (2005)
- 30- Sharma A, Sharma R, Chaudhary P, Vatsyayan R, Pearce V, Jeyabal PV, et al. 4-Hydroxynonenal induces p53-mediated apoptosis in retinal pigment epithelial cells. *Arch Biochem Biophys* 480(2):85-94 (2008)
- 31- Choudhary S, Xiao T, Srivastava S, Zhang W, Chan LL, Vergara LA, et al. Toxicity and detoxification of lipid-derived aldehydes in cultured retinal pigmented epithelial cells. *Toxicol Appl Pharmacol* 204(2):122-34 (2005)
- 32- Vatsyayan R, Chaudhary P, Sharma A, Sharma R, Rao Lelsani PC, et al. Role of 4-hydroxynonenal in epidermal growth factor receptor-mediated signaling in retinal pigment epithelial cells. *Exp Eye Res* 92(2):147-54 (2011)
- 33- Weigel AL, Handa JT, Hjelmeland LM. Microarray analysis of H₂O₂-, HNE-, or tBH-treated ARPE-19 cells. *Free Radic Biol Med* 33(10):1419-32 (2002)

- 34- Bergmann M, Holz F, Kopitz J. Lysosomal stress and lipid peroxidation products induce VEGF 121 and VEGF-165 expression in ARPE-19 cells. *Graefes Arch Clin Exp Ophthalmol* 249(10):1477-83 (2011)
- 35- Scheper W, Hoozemans JJ. The unfolded protein response in neurodegenerative diseases: a neuropathological perspective. *Acta Neuropathol* 130(3):315-31. doi: 10.1007/s00401-015-1462-8 (2015)
- 36- Volgyi K, Juhász G, Kovacs Z, Penke B. Dysfunction of Endoplasmic Reticulum (ER) and Mitochondria (MT) in Alzheimer's Disease: The Role of the ER-MT Cross-Talk. *Curr Alzheimer Res* 12(7):655-72 (2015)
- 37- Libby RT, Gould DB. Endoplasmic reticulum stress as a primary pathogenic mechanism leading to age-related macular degeneration. *Adv Exp Med Biol* 664:403-9 (2010)
- 38- Wu M, Yang S, Elliott MH, Fu D, Wilson K, Zhang J, et al. Oxidative and endoplasmic reticulum stresses mediate apoptosis induced by modified LDL in human retinal Müller cells. *Invest Ophthalmol Vis Sci* 53(8):4595-604 (2012)
- 39- Takahashi K, Niidome T, Akaike A, Kihara T, Sugimoto H. Amyloid precursor protein promotes endoplasmic reticulum stress-induced cell death via C/EBP homologous protein-mediated pathway. *J Neurochem* 109(5):1324-37 (2009)
- 40- Copanaki E, Schürmann T, Eckert A, Leuner K, Müller WE, Prehn JH, et al. The amyloid precursor protein potentiates CHOP induction and cell death in response to ER Ca²⁺ depletion. *Biochim Biophys Acta* 1773(2):157-65 (2007)
- 41- Kögel D, Schomburg R, Schürmann T, Reimertz C, König HG, Poppe M, et al. The amyloid precursor protein protects PC12 cells against endoplasmic reticulum stress-induced apoptosis. *J Neurochem* 87:248-56 (2003)
- 42- Kögel D, Schomburg R, Copanaki E, Prehn JH. Regulation of gene expression by the amyloid precursor protein: inhibition of the JNK/c-Jun pathway. *Cell Death Differ* 12:1-9 (2005)
- 43- Masliah E, Westland CE, Rockenstein EM, Abraham CR, Mallory M, Veinberg I, et al. Amyloid precursor proteins protect neurons of transgenic mice against acute and chronic excitotoxic injuries in vivo. *Neuroscience* 8(1):135-46 (1997)
- 44- Chen ST, Gentleman SM, Garey LJ, Jen LS. Distribution of beta-amyloid precursor and B-cell lymphoma protooncogene proteins in the rat retina after optic nerve transection or vascular lesion. *J Neuropathol. Exp Neurol* 55(10):1073-82 (1996)
- 45- McGillem GS, Dacheux RF. Rabbit retinal Müller cells undergo antigenic changes in response to experimentally induced proliferative vitreoretinopathy. *Exp Eye Res* 68(5):617-27 (1999)
- 46- Yoshida T, Fukatsu R, Tsuzuki K, Aizawa Y, Hayashi Y, Sasaki N, et al. Amyloid precursor protein, A beta and amyloid-associated proteins involved in chloroquine retinopathy in rats.

Brain Res 764(1-2):283-8 (1997)

47- Limb GA, Salt TE, Munro PM, Moss SE, Khaw PT. In vitro characterization of a spontaneously immortalized human Müller cell line (MIO-M1). Invest Ophthalmol Vis Sci 43:864-9 (2002)

48- Glotin AL, Debaq-Chainiaux F, Brossas JY, Faussat AM, Treton J, Zubielewicz A, et al. Prematurely senescent ARPE-19 cells display features of age-related macular degeneration. Free Radic Biol Med 44: 1348-61 (2008)

49- Mucke L, Abraham CR, Masliah E. Neurotrophic and neuroprotective effects of hAPP in transgenic mice. Ann N Y Acad Sci 777:82-8 (1996)

50- Schubert D, Behl C. The expression of amyloid beta protein precursor protects nerve cells from beta-amyloid and glutamate toxicity and alters their interaction with the extracellular matrix. Brain Res 629(2):275-82 (1993)

51- Esposito L, Gan L, Yu GQ, Essrich C, Mucke L. Intracellularly generated amyloid-beta peptide counteracts the antiapoptotic function of its precursor protein and primes proapoptotic pathways for activation by other insults in neuroblastoma cells. J Neurochem. 91(6):1260-74 (2004)

52- Zhao Z, Chen Y, Wang J, Sternberg P, Freeman ML, Grossniklaus HE, et al. Age-related retinopathy in NRF2-deficient mice. PLoS One 6(4):e19456 (2011)

53- Liu X, Ward K, Xavier C, Jann J, Clark AF, Pang IH, et al. The novel triterpenoid RTA 408 protects human retinal pigment epithelial cells against H₂O₂-induced cell injury via NF-E2 related factor 2 (Nrf2) activation. Redox Biol 8:98-109 (2016)

54- Chen WJ, Wu C, Xu Z, Kuse Y, Hara H, Duh EJ. Nrf2 protects photoreceptor cells from photo oxidative stress induced by blue light. Exp Eye Res 154:151-158 (2016)

55- Xiong W, MacColl Garfinkel AE, Li Y, Benowitz LI, Cepko CL. NRF2 promotes neuronal survival in neurodegeneration and acute nerve damage. J Clin Invest 125(4):1433-45 (2015)

56- Deliyanti D, Lee JY, Petratos S, Meyer CJ, Ward KW, Wilkinson-Berka JL, et al. A potent Nrf2 activator, dh404, bolsters antioxidant capacity in glial cells and attenuates ischaemic retinopathy. Clin Sci (Lond)130(15):1375-87 (2016)

57- Shih AY, Johnson DA, Wong G, Kraft AD, Jiang L, Erb H, et al. Coordinate regulation of glutathione biosynthesis and release by Nrf2-expressing glia potently protects neurons from oxidative stress. J Neurosci 23(8):3394-406 (2003)

58- Joshi G, Gan KA, Johnson DA, Johnson JA. Increased Alzheimer's disease-like pathology in the APP/ PS1ΔE9 mouse model lacking Nrf2 through modulation of autophagy. Neurobiol. Aging 36(2):664-79 (2015)

59- Kanninen K, Heikkinen R, Malm T, Rolova T, Kuhmonen S, Leinonen H, et al. Intrahippocampal injection of a lentiviral vector expressing Nrf2 improves spatial learning in a mouse model of

Alzheimer's disease. *Proc. Natl Acad Sci U S A* 106(38):16505-10 (2009)

60- Ryoo HD, Domingos PM, Kang MJ, Steller H. Unfolded protein response in a *Drosophila* model for retinal degeneration. *EMBO J* 26(1):242-52 (2007)

61- Chen C, Cano M, Wang JJ, Li J, Huang C, Yu Q, et al. Role of unfolded protein response dysregulation in oxidative injury of retinal pigment epithelial cells. *Antioxid Redox Signal* 20(14):2091-106 (2014)

62- Huang C, Wang JJ, Ma JH, Jin C, Yu Q, Zhang SX. Activation of the UPR protects against cigarette smoke-induced RPE apoptosis through up-regulation of Nrf2. *J Biol Chem* 290(9):5367-80 (2015)

63- Zhong Y, Li J, Wang JJ, Chen C, Tran JT, Saadi A, et al. X-box binding protein 1 is essential for the anti-oxidant defense and cell survival in the retinal pigment epithelium. *PLoS One* 7(6):e38616 (2012)

64- Reinhardt S, Schuck F, Grösgen S, Riemenschneider M, Hartmann T, Postina R, et al. Unfolded protein response signaling by transcription factor XBP-1 regulates ADAM10 and is affected in Alzheimer's disease. *FASEB J* 28(2):978-97 (2014)

65- Loewen CA, Feany MB. The unfolded protein response protects from tau neurotoxicity in vivo. *PLoS One* 29 5(9) (2010)

66- Casas-Tinto S, Zhang Y, Sanchez-Garcia J, Gomez-Velazquez M, Rincon-Limas DE, Fernandez Funez P. The ER stress factor XBP1s prevents amyloid-beta neurotoxicity. *Hum Mol Genet* 20:2144-60 (2011)

67- Mota SI, Costa RO, Ferreira IL, Santana I, Caldeira GL, Padovano C, et al. Oxidative stress involving changes in Nrf2 and ER stress in early stages of Alzheimer's disease. *Biochim Biophys Acta* 1852(7):1428-41 (2015)

68- Mendes CS, Levet C, Chatelain G, Dourlen P, Fouillet A, Dichtel-Danjoy ML, et al. ER stress protects from retinal degeneration. *EMBO J* 28(9):1296-307 (2009)

69- Zhang T, Zhang N, Baehr W, Fu Y Cone opsin determines the time course of cone photoreceptor degeneration in Leber congenital amaurosis. *Proc Natl Acad Sci U S A*. 24;108(21):8879-84 (2011)

70- Joly S, Lamoureux S, Pernet V. Nonamyloidogenic processing of amyloid beta precursor protein is associated with retinal function improvement in aging male APP^{swe}/PS1^{ΔE9} mice. *Neurobiol Aging* 181-191 (2017)

LEGENDS TO FIGURES

Figure 1. HNE induced oxidative stress and mitochondrial dysfunction in MC cultures.

Production of extracellular ROS (A) was measured with H2DCFDA and FACS analysis; intracellular redox potential (B) was analyzed by the Alamar blue test; mitochondrial redox potential (C) was analyzed by the MTT colorimetric assay; mitochondrial transmembrane potential (D) was measured with the JC-1 probe; and the cardiolipin level (E) was quantified with the NOA probe. The percentages by which intracellular redox, potential mitochondrial redox potential and mitochondrial transmembrane potential decreased and cardiolipin level increased were calculated relative to vehicle treated control cells. Similar results were obtained in three independent experiments. Asterisks indicate significant differences (* $p < 0.05$).

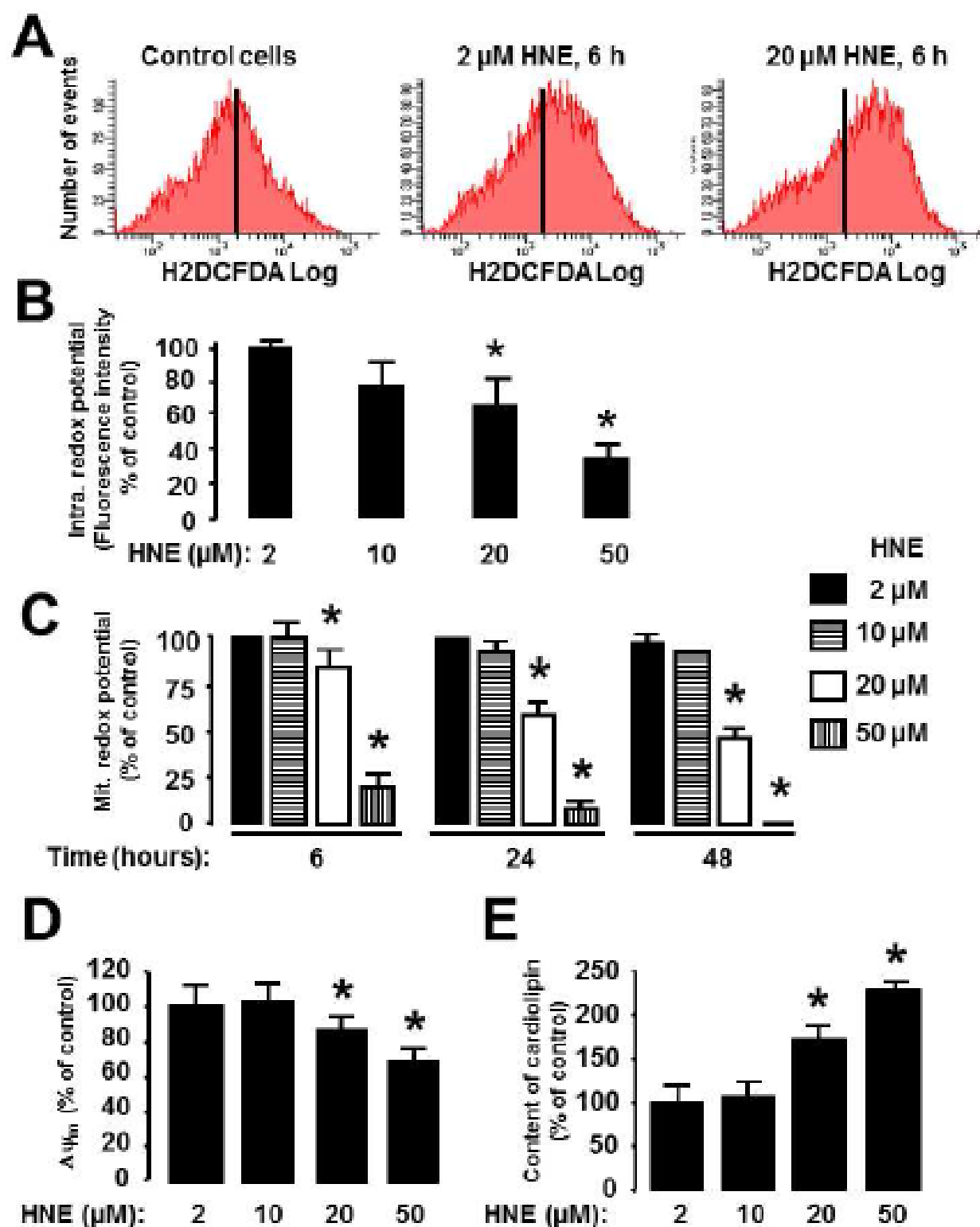
Figure 2. HNE induced plasma membrane damage and apoptosis in MC cultures. Damage to the plasma membrane (A) was assessed by the LDH activity release assay; and cell viability (B) was quantified by counting trypan blue-excluding cells; the sub-G1 peak (C) was analyzed by FACS after propidium iodide (PI) staining; and apoptosis (D) was detected by the TUNEL method after 24h of HNE treatment. The percentages of membrane damage and of the reduction in cell survival were calculated relative to vehicle-treated control cells. SD error bar does not appear when smaller than the symbol. Similar results were obtained in three independent experiments. Asterisks indicate significant differences (* $p < 0.05$).

Figure 3. Effects of A β PP overexpression on oxidative stress and cell survival in HNE-treated MC. Cultures of MCapp, MCpc and MC were or were not treated with HNE (20 μ M); mitochondrial redox potential (A) was analyzed by the MTT colorimetric assay; cell viability (B) was assessed by counting trypan blue-excluding cells. SD error bar does not appear when smaller than the symbol. Similar results were obtained in three independent experiments. Asterisks indicate significant differences (* $p < 0.05$).

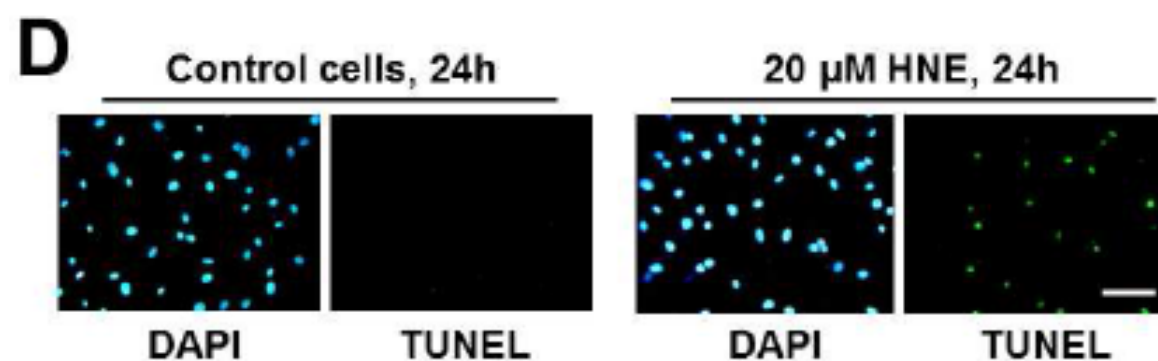
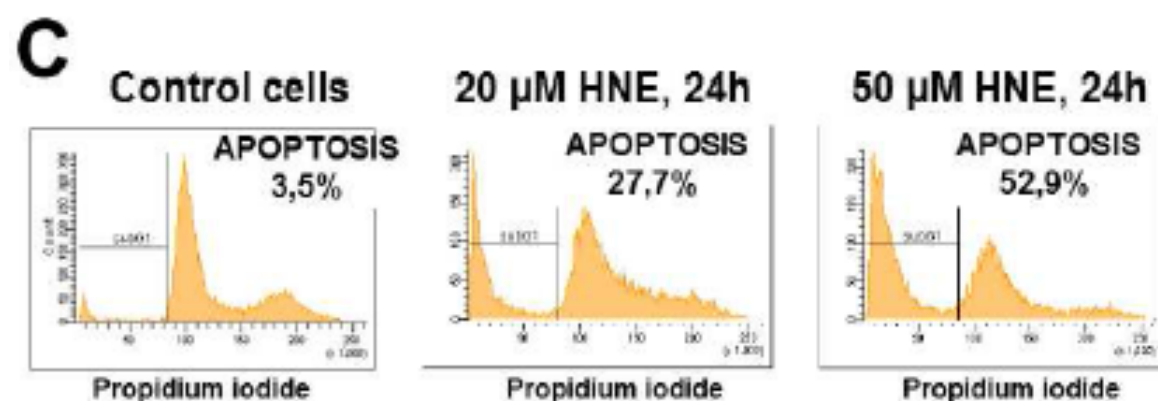
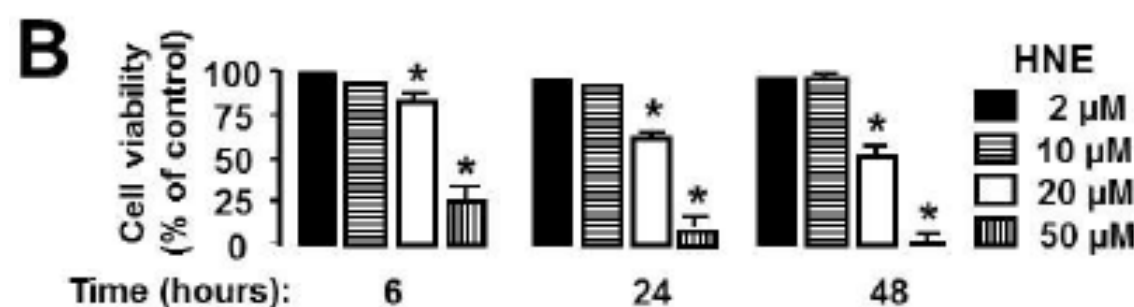
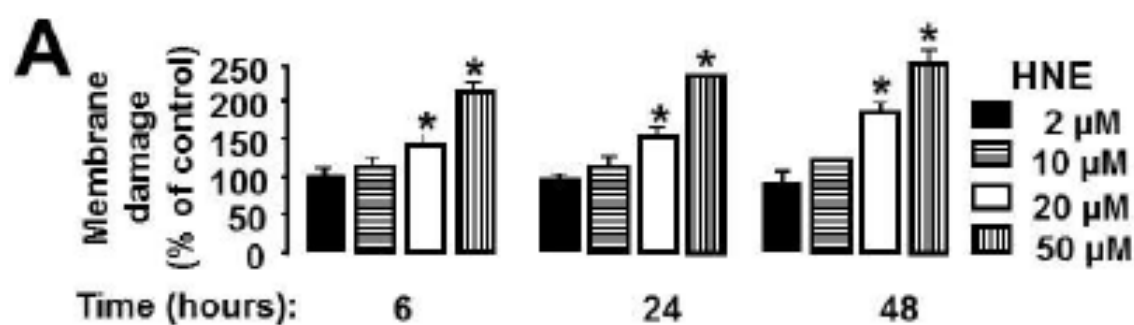
Figure 4. Schematic representation of the effects of HNE on the various effectors studied in the different pathways. HNE-mediated oxidative stress was associated with ER stress and alteration of the retinal homeostatic function of MC. Overexpression of A β PP induced a specific response by activating ERAD, a strong antioxidant defense, the restoration of expression of major genes involved in retinal homeostasis and downregulation of ER stress. A β PP had no effect on inflammation.

Table 1. Identification of HNE-induced changes in gene expression in MC. Twenty-two genes related to MC function, angiogenesis, inflammation, and amyloidogenesis were studied to investigate the effects of HNE (20 μ M) on MC homeostasis after 6 h of culture. The expression levels of genes in HNE-treated cell group were compared to the control group and a value for fold-change in expression was generated. (–) Indicates lower expression in the HNE-treated cell group. Data are the mean \pm SD. Asterisks indicate significant difference (* $p < 0.05$).

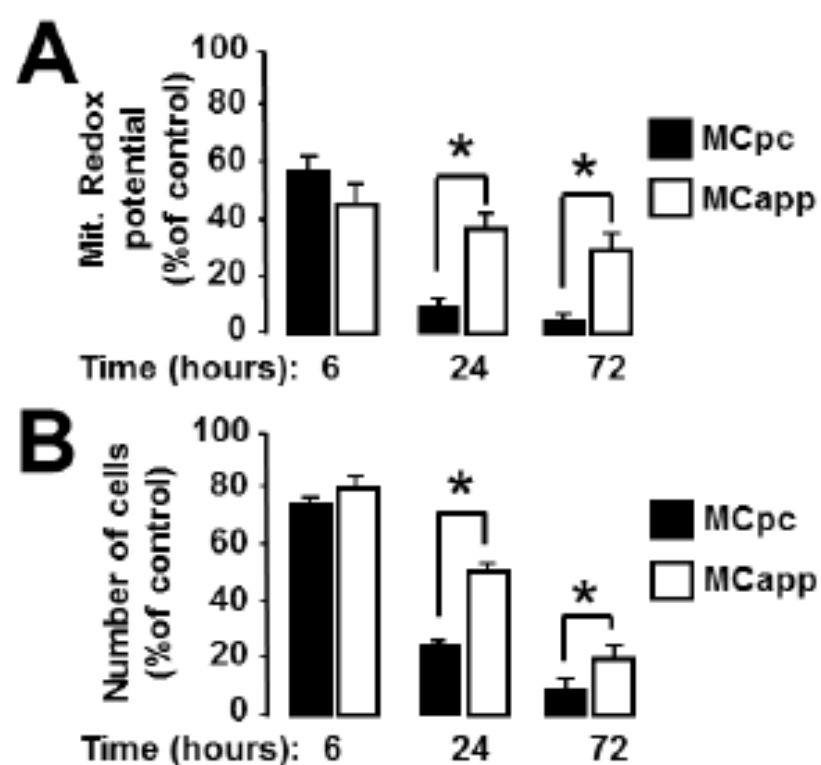
Table 2. Effects of A β PP overexpression on gene expression in MC. Twenty-six genes related to ER stress, oxidative stress, and MC functions were studied to investigate the effects of A β PP overexpression on MC homeostasis after 3 days of culture. The expression levels of genes in the MCapp cell group were compared to the control MCpc cell group and a value for fold-change in expression was generated. (–) Indicates lower expression in the MCapp cell group. Data are the mean \pm SD. Asterisks indicate significant difference (*p < 0.05).



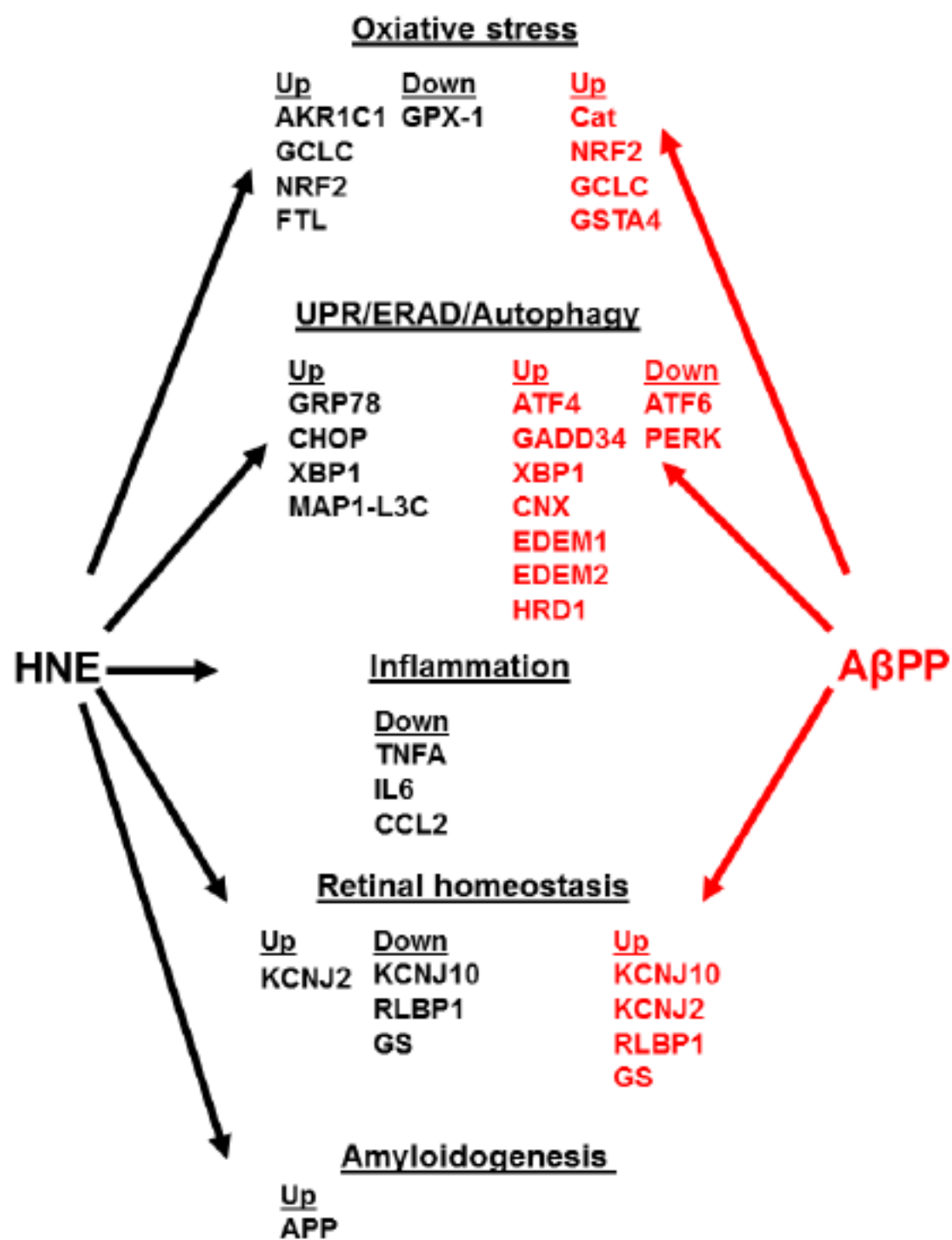
Chalouret *et al.*, Fig. 1



Chalouret *et al.*, Fig. 2



Chalour et al., Fig. 3



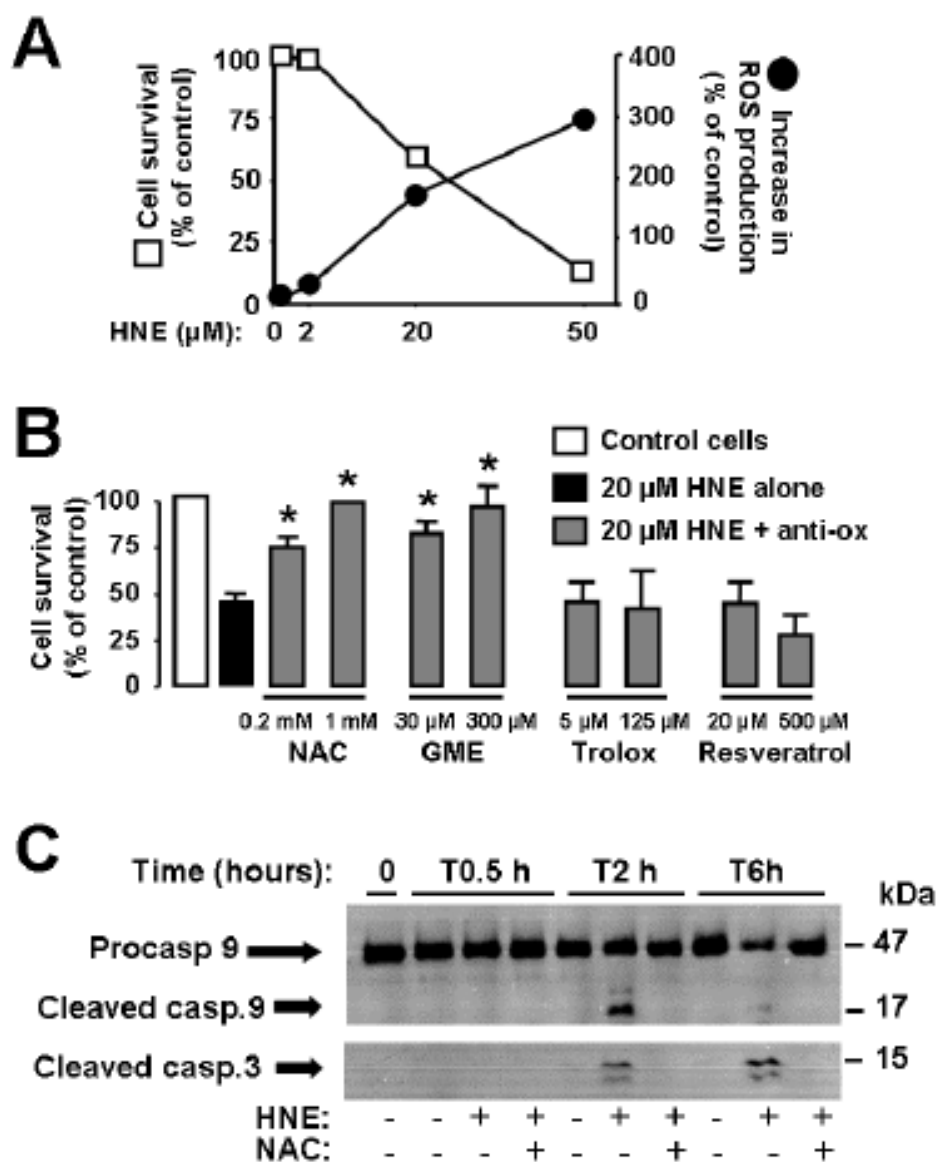
Chalour et al., Fig. 4

Gene symbol	Gene name	Change (fold)
<u>Oxidative stress</u>		
CAT	Catalase	1.0 ± 0.1
SOD1	Superoxide dismutase 1	1.2 ± 0.1
SOD2	Superoxide dismutase 2	1.0 ± 0.1
GPX-1	Glutathione peroxidase	-1.3 ± 0.1 [*]
AKR1C1	Aldo-keto reductase 1C family member 1	1.9 ± 0.3 [*]
GCLC	Glutamate cysteine ligase catalytic subunit	2.3 ± 0.5 [*]
GSTA4	Glutathione S-transferase-α.4	1.4 ± 0.2
NRF2	Nuclear factor erythroid-derived 2, like 2	1.3 ± 0.1 [*]
<u>UPR</u>		
GRP78	78 kDa glucose-regulated protein/ Binding immunoglobulin protein (BiP)	1.5 ± 0.1 [*]
ATF4	Activating transcription factor 6	1.6 ± 0.4
CHOP	C/EBP homologous protein	2.7 ± 0.3 [*]
ATF6	Activating transcription factor 6	1.1 ± 0.2
IRE1	Inositol-requiring enzyme 1	1.5 ± 0.2
XBP1	Unspliced form of X-box binding protein 1	2.0 ± 0.3 [*]
XBP1s	Spliced form of X-box binding protein 1	2.2 ± 0.3 [*]
GADD34	Growth arrest and DNA damage inducible protein 34	2.0 ± 0.4
<u>ERAD</u>		
CNX	Calnexin	1.0 ± 0.1
EDEM1	ER degradation-enhancing alpha-Mannosidase-like protein 1	1.0 ± 0.1
EDEM2	ER degradation-enhancing alpha-Mannosidase-like protein 2	1.0 ± 0.1
HRD1	ERAD-associated E3 ubiquitin-protein ligase	1.3 ± 0.2
<u>Autophagy</u>		
MAP1-L3C	Microtubule-associated protein 1 light chain 3	2.1 ± 0.4 [*]
ATG5	Autophagy Related 5 Homolog	1.2 ± 0.2
BECN1	Beclin-1	1.0 ± 0.1
<u>Amyloidogenesis</u>		
APP	β-amyloid protein precursor	1.4 ± 0.1 [*]
APP770	β-amyloid protein precursor 770	1.3 ± 0.1 [*]
APOE	Apolipoprotein E	1.0 ± 0.2

Chalouret *et al.*, Table 1

Gene symbol	Gene name	Change (fold)
APP	Amyloid protein precursor	$1.9 \pm 0.5^*$
APP-KPI	Amyloid protein precursor kunitz protease inhibitor domain	$1.9 \pm 0.5^*$
<u>UPR</u>		
GRP78	78 kDa glucose-regulated protein/ Binding immunoglobulin protein (BiP)	-1.3 ± 0.2
PERK	PKR-like ER kinase	$-1.9 \pm 0.2^*$
ATF4	Activating transcription factor 4	$1.4 \pm 0.1^*$
GADD34	Growth arrest and DNA damage protein 34	$2.4 \pm 0.2^*$
CHOP	C/EBP homologous protein	1.1 ± 0.1
ATF6	Activating transcription factor 6	$-1.3 \pm 0.1^*$
IRE1	Inositol-requiring enzyme 1	-1.1 ± 0.1
XBP1	X-box binding protein 1	$2.1 \pm 0.3^*$
XBP1-s	Spliced X-box binding protein 1	$4.0 \pm 0.2^*$
<u>ERAD</u>		
CNX	Calnexin	$2.1 \pm 0.3^*$
EDEM1	ER degradation-enhancing alpha-mannosidase-like protein 1	$1.8 \pm 0.1^*$
EDEM2	ER degradation-enhancing alpha-mannosidase-like protein 2	$2.3 \pm 0.4^*$
HRD1	ERAD-associated E3 ubiquitin-protein ligase	$1.4 \pm 0.1^*$
<u>Oxidative stress</u>		
CAT	Catalase	$3.7 \pm 0.4^*$
SOD1	Superoxide dismutase 1	1.3 ± 0.3
SOD2	Superoxide dismutase 2	-1.2 ± 0.2
GPX-1	Glutathione peroxidase	-1.0 ± 0.1
NRF2	Nuclear factor erythroid-derived 2, like 2	$7.5 \pm 0.3^*$
GCLC	Glutamate cysteine ligase catalytic subunit	$2.0 \pm 0.2^*$
GSTA4	Glutathione S-transferase- α 4	$2.7 \pm 0.5^*$
<u>Retinal homeostasis</u>		
KCNJ2	Potassium inwardly-rectifying channel 2.1	$5.2 \pm 0.5^*$
KCNJ10	Potassium inwardly-rectifying channel 4.1	$5.1 \pm 0.7^*$
GS	Glutamine synthetase	$2.1 \pm 0.4^*$
RLBP1	Cellular retinaldehyde binding protein	$1.7 \pm 0.1^*$

Chalour et al., Table 2



Supplementary Fig. S1: HNE induced GSHdependent and caspaseassociated apoptosis of MC cultures.

(A) Cell viability was assessed by counting trypan blueexcluding cells, and production of extracellular ROS was measured with H2DCFDA and FACS analysis. The effect of HNE on ROS production was analyzed together with cell viability; using the trypan blueexclusion assay. Similar results were obtained in three independent experiments. (B) The effects on cell viability of pretreatment (one hour before stimulation with HNE (20 μM)) with different antioxidant chemicals were analyzed after 24 h of culture, by the trypan blueexclusion assay. The percentage of cell survival was calculated relative to vehicle-treated control cells. Similar results were obtained in two independent experiments. Asterisks indicate significant differences (*p < 0.05). (C) The activation of caspase 3 and caspase 9 was detected

by western blotting. The effects of pretreatment (one hour before stimulation with HNE (20 μ M)) with NAC (1 mM) on caspase cleavage were analyzed.

Intracellular production of ROS in MC cells was inversely correlated with cell survival

during HNE treatment: at 2 μ M, HNE had almost no effects on the stimulation of ROS

production over a 24-h culture period and no significant effects on cell viability (Fig. S1A). In

contrast, treatment with 20 μ M HNE induced a 1.8-fold increase in ROS production and a

38% reduction in cell viability after 24 h of culture; after the same period, 50 μ M HNE

induced a 3.1-fold increase in ROS production and reduced cell viability by 78% (Fig. S1A).

Accordingly, we characterized the mechanism of HNE-induced MC cell death by studying the

protective antioxidant pathways. Pretreatment with 0.2 mM N-acetylcystein (NAC), a GSH

precursor, reduced the effects of 20 μ M HNE on cell viability by 46%, and at a concentration

of 1 mM it completely blocked this lethal effect (Fig. S1B). Cell treatment with glutathione

monoethyl ester (GME), a GSH analog, greatly reduced cell death (56% reduction with 30 μ M

GME and 91% reduction with 300 μ M GME) 24 h after treatment with 20 μ M HNE. This

finding indicated the role of the GSH pathway in the antioxidant defense of MC (Fig. S1B). In

contrast, cell treatment with trolox (5-125 μ M), a derivative of vitamin E that acts as a free

radical scavenger or with the flavonoid resveratrol (20-500 μ M) did not reverse the lethal

effect of 20 μ M HNE (Fig. S1B). Western blot analysis was then used to assess the protective

effects of NAC against HNE-induced activation of caspase 3 and 9. HNE induced caspase-9

activation, as revealed by the cleavage of procaspase-9 (47 kDa) into the active 17-kDa

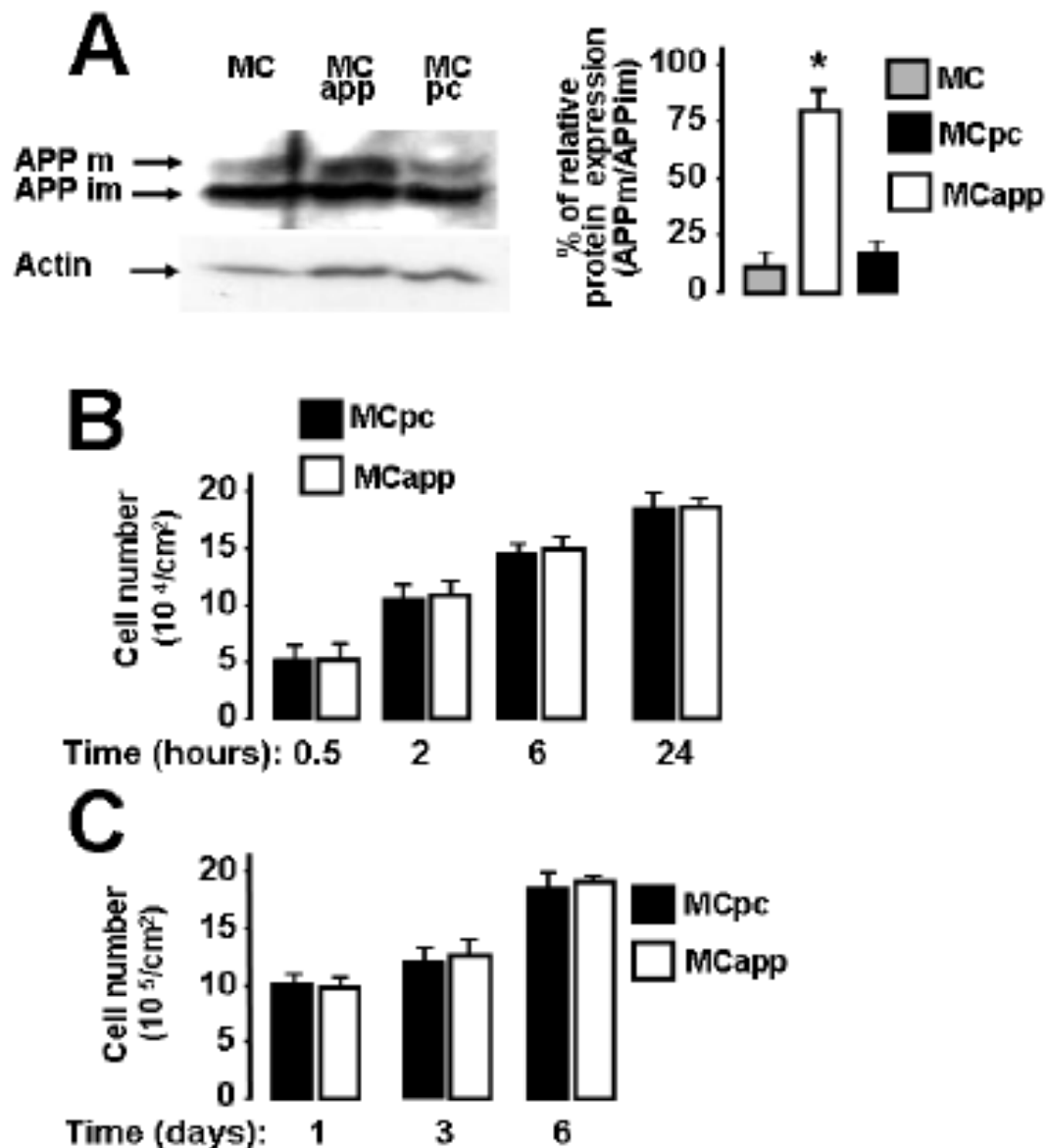
fragment 2 h after HNE treatment (Fig. 6C). Sustained cleavage of the inactive form of

caspase-3 into the active 17- and 12-kDa fragments was also observed after 2 h and over a 6-h

treatment period (Fig. S1C). Treatment with 1 mM NAC completely blocked both the HNE

induced cleavage of procaspase-9 and procaspase-3 (Fig. S1C), thereby confirming that the

GSH pathway protects MC from the lethal effect of HNE. Together these data indicate that HNE induces glutathione-dependent and activated caspase-associated apoptosis of MC.



Supplementary Fig. S2: Effects of stable overexpression of A β PP on cell adhesion and cell proliferation in MC cultures. (A) Expression levels of the mature form of A β PP (APP m) and of the immature form of A β PP (APP im) were investigated by western blotting with an antiCt A β PP antibody (CT"2, Calbiochem). Cell adhesion (B) and basal cell proliferation (C) were investigated. Similar results were obtained in three independent experiments.

At moderate levels of sustained overexpression, human A β PP protects cell lines and transgenic mice against oxidative stress and increases resistance to excitotoxicity [1-4]. However, the exact mechanism of these protective effects remains largely unknown. In line with these findings and our data showing moderate upregulation of A β PP in HNE-treated MC, we hypothesized that upregulation of A β PP is an adaptive process to protect MC against lethal HNE-induced oxidative stress.

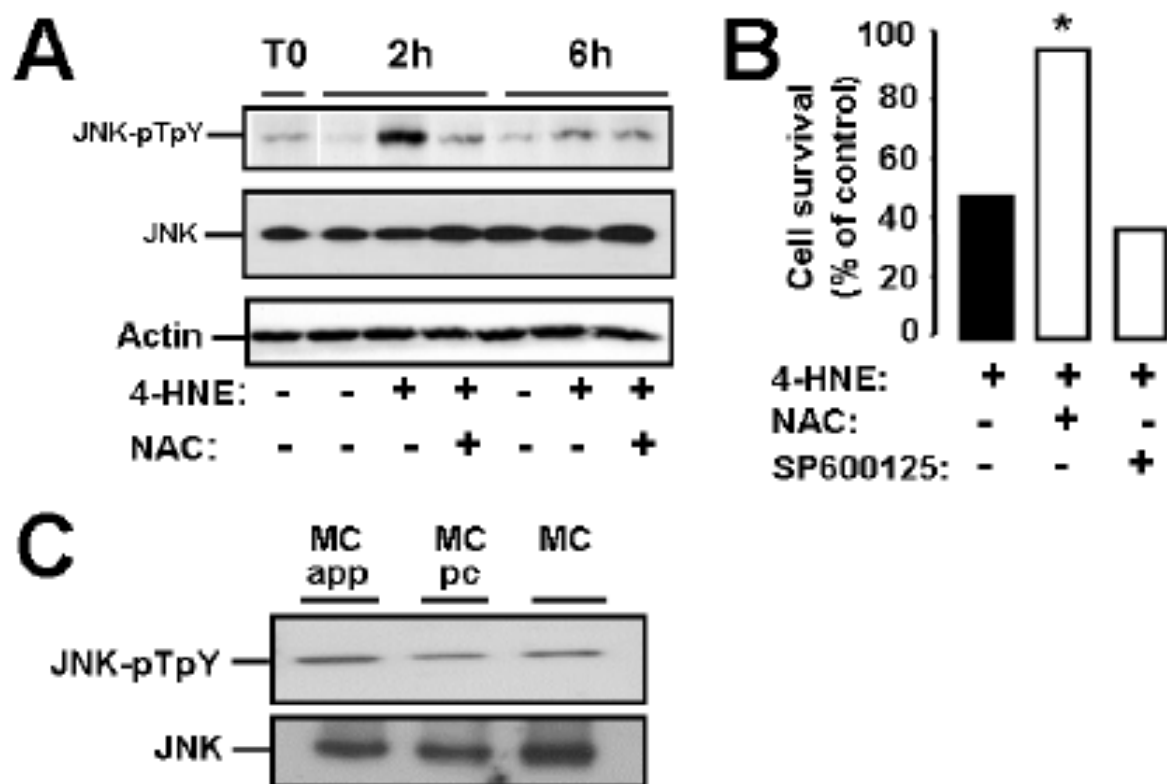
To test this hypothesis, we stably transfected MC cells with the pc-DNA-APP695 expression vector (MCapp cells) or with the pc-DNA3 empty vector (MCpc cells), as a control. Compared with the control MCpc cells, the MCapp cells stably overexpressed APP mRNA (by a factor of 1.9) (Table 3) as well as the mature form of A β PP protein (Fig. S2A). Preliminary experiments showed that overexpression of A β PP in MC did not affect either cell adhesion (Fig. S2B) or cell proliferation (Fig. S2C) and thereby suggested that A β PP overexpression does not affect the overall comportment of MC in normal conditions.

[1] Kögel D, Schomburg R, Schürmann T, Reimertz C, König HG, Poppe M, et al. The amyloid precursor protein protects PC12 cells against endoplasmic reticulum stress-induced apoptosis. *J Neurochem* 87:248-56 (2003)

[2] Kögel D, Schomburg R, Copanaki E, Prehn JH. Regulation of gene expression by the amyloid precursor protein: inhibition of the JNK/c-Jun pathway. *Cell Death Differ* 12:1-9 (2005)

[3] Masliah E, Westland CE, Rockenstein EM, Abraham CR, Mallory M, Veinberg I, et al. Amyloid precursor proteins protect neurons of transgenic mice against acute and chronic excitotoxic injuries in vivo. *Neuroscience* 8(1):135-46 (1997)

[4] Chen ST, Gentleman SM, Garey LJ, Jen LS. Distribution of beta-amyloid precursor and B-cell lymphoma protooncogene proteins in the rat retina after optic nerve transection or vascular lesion. *J. Neuropathol. Exp Neurol* 55(10):1073-82 (1996)



Supplementary Fig. S3: Overexpression of A β PP did not activate JNK in MC cultures. (A) The levels of JNK phosphorylation (JNKpTpY) were detected by western blotting. (B) The effect of pretreatment (30 min before stimulation with HNE (20 μ M)) with the specific inhibitor of JNK (SP600125, 20 μ M) on cell viability of MC was analyzed after 48 h of culture, with the trypan blue exclusion assay. The percentage of cell survival was calculated relative to vehicle-treated control cells. (D) The levels of JNK phosphorylation (JNKpTpY) in MCapp and MCpc cells were detected by western blotting. Similar results were obtained in three independent experiments.

Gene symbol	Gene name	Change (fold)
<u>Retinal homeostasis</u>		
KCNJ2	Potassium inwardly-rectifying channel 2.1	1.8 ± 0.4 [*]
KCNJ10	Potassium inwardly-rectifying channel 4.1	-1.5 ± 0.2 [*]
EAAT-1	L-glutamate transporters -1	1.0 ± 0.1
GS	Glutamine synthetase	-1.4 ± 0.1 [*]
RLBP1	Cellular retinaldehyde binding protein	-2.2 ± 0.2 [*]
CA9	Carbonic anhydrase 9 transporter	-1.1 ± 0.4
<u>Gliosis</u>		
VIM	Vimentin	1.1 ± 0.1
GFAP	Glial fibrillary acidic protein	-1.6 ± 0.2
NES	Nestin	1.1 ± 0.1
<u>Inflammation</u>		
TNFA	Tumor necrosis factor α	-4.8 ± 0.1 [*]
IL1B	Interleukin 1 β	-1.4 ± 0.3
IL6	Interleukin 6	-1.7 ± 0.2 [*]
IL8	Interleukin 8	1.0 ± 0.1
CCL2	CC chemokine ligand 2	-2.1 ± 0.4 [*]
FH	Complement factor H	1.0 ± 0.2
COX1	Cytochrome oxidase-1	1.0 ± 0.3
COX2	Cytochrome oxidase-2	1.2 ± 0.3
<u>Angiogenesis</u>		
VEGF	Vascular endothelial growth factor	1.0 ± 0.2
PEDF	Pigment epithelium-derived factor	1.1 ± 0.3

Supplementary Table S1: MC elicit a specific transcriptional program in response to HNE, with the induction of antiinflammatory genes, together with impairment of retinal homeostasis genes. Nineteen genes related to oxidative stress, UPR, ERAD, and autophagy were tested to investigate the effects of HNE (20 μ M) on ER stress in MC after 6 h of culture. The expression levels of genes in HNE-treated cell group were compared to the control group and a value for foldchange in expression was generated. (–) Indicates lower expression in the HNE-treated cell group. Data are the mean \pm SD. Asterisks indicate significant difference (*p < 0.05).